Robust IDA-PBC for underactuated mechanical systems subject to matched disturbances

Alejandro Donaire[1,4,*,†], Jose Guadalupe Romero[2], Romeo Ortega[3],
Bruno Siciliano[1] and Martin Crespo[5]

[1]*PRISMA Lab, Dipartimento di Ingegneria Elettrica e Tecnologie dell'Informazione, Università di Napoli Federico II, 80125 Naples , Italy*
[2]*Departamento Académico de Sistemas Digitales, Instituto Tecnológico Autónomo de México-ITAM, Federal District, México*
[3]*Laboratoire des Signaux et Systèmes, CNRS-SUPELEC, 91192 Gif-sur-Yvette, France*
[4]*School of Engineering, The University of Newcastle, Callaghan, NSW, Australia*
[5]*Departamento de Control, FCEIA, Universidad Nacional de Rosario, Rosario, Argentina*

SUMMARY

The problem of robustification of interconnection and damping assignment passivity-based control for underactuated mechanical system *vis-à-vis* matched, constant, and unknown disturbances is addressed in the paper. This is achieved adding an outer-loop controller to the interconnection and damping assignment passivity-based control. Three designs are proposed, with the first one being a simple nonlinear PI, while the second and the third ones are nonlinear PIDs. While all controllers ensure stability of the desired equilibrium in spite of the presence of the disturbances, the inclusion of the derivative term allows us to inject further damping enlarging the class of systems for which asymptotic stability is ensured. Numerical simulations of the Acrobot system and experimental results on the disk-on-disk system illustrate the performance of the proposed controller. Copyright © 2016 John Wiley & Sons, Ltd.

1. INTRODUCTION

Interconnection and damping assignment passivity-based control (IDA-PBC), first introduced in [1], is a highly popular controller design technique applicable for equilibrium stabilization of a wide class of physical systems (e.g., [2–6]). A comprehensive discussion of IDA-PBC may be found in [7]. Its application for underactuated mechanical systems has been particularly successful as reported, for instance, in [8–11]. It is widely recognized that IDA-PBC designs are robust against parameter uncertainties and unmodelled dynamics, for example, passive effects like friction. However, the (unavoidable) presence of external disturbances degrades its performance, shifting the equilibrium of the closed loop and, possibly, inducing instability. For this reason, the problem of robustification of IDA-PBC *vis-à-vis* external disturbances is of primary importance.

For fully actuated mechanical systems, this problem has been addressed in [12], where the key idea of adding an integral action that preserves the port-Hamiltonian (pH) structure of the system, first proposed in [13], is exploited. Proposition 5 of [12] presents a dynamic nonlinear controller, including the essential integral action, that ensures global asymptotic stability of the desired equi-

librium in spite of the presence of constant matched disturbances. The case of unmatched and/or time-varying disturbances is also studied in that paper, where controllers that ensure input-state-stability are proposed. In [14], the addition of integral action in velocities for the particular case of constant mass matrix is considered. However, the integral action in velocities does not reject matched disturbances and creates a manifold of equilibrium, as indicated in [12].

To the best of the authors' knowledge, the first attempt to solve the constant, disturbance rejection problem for underactuated mechanical systems was published in [15]. The authors consider the simplest case of two DOF mechanical systems with constant mass matrix and underactuation degree one. Although the main idea is interesting, there are several unfortunate errors that invalidate the claims. Indeed, it is easy to show that the proposed control law, given in Equation (27) of [15], does not satisfy the matching equations, which is a key step in the design. Moreover, because it is not possible to inject damping in all the momentum coordinates, the closed-loop damping matrix is not full rank, a critical assumption made in [15] to claim asymptotic stability.

In this paper, we complement the main idea of [15], that is adding an integral action on non-passive outputs of underactuated systems, with the developments of [12] to propose an outer-loop controller that solves the problem of (constant and matched) disturbance rejection for underactuated n-DOF mechanical systems with arbitrary underactuation degree. An interesting feature of the proposed outer loops is that they do not destroy the mechanical structure of the system, preserving in closed loop its pH form. The design is applicable for systems where the mass matrix is independent of the unactuated coordinates and the closed-loop mass matrix is constant. The first assumption is instrumental for the results reported in [8, 9, 11], where it is imposed to simplify the kinetic energy matching equation. In the present work, this assumption, as well as the requirement that the closed-loop mass matrix is constant, are needed to construct a suitable change of coordinates under which the integral action is added. It should be noted that these assumptions are verified by a large class of underactuated mechanical systems, including those considered in [9].

The rest of the paper is organized as follows. Section 2 briefly recalls IDA-PBC and formulates its robustification problem. The main result of the paper is presented in Section 3. The performance of the controller is illustrated in Section 4 with numerical simulations of the Acrobot [9] and in Section 5 with experimental results of the disk-on-disk system [21]. Future work is discussed in Section 6.

Notation. For $x \in \mathbb{R}^n$, $S \in \mathbb{R}^{n \times n}$, $S = S^\top > 0$, we denote $|x|^2 := x^\top x$ and $\|x\|_S^2 := x^\top S x$. Given a function $H : \mathbb{R}^n \to \mathbb{R}$ we define $\nabla H := \left(\frac{\partial H}{\partial x} \right)^\top$.

2. ROBUST INTERCONNECTION AND DAMPING ASSIGNMENT PASSIVITY-BASED CONTROL

2.1. Standard interconnection and damping assignment passivity-based control

Interconnection and damping assignment passivity-based control was introduced in [10] to control underactuated mechanical systems described in pH form

$$\begin{bmatrix} \dot{q} \\ \dot{p} \end{bmatrix} = \begin{bmatrix} 0_{n \times n} & I_n \\ -I_n & 0_{n \times n} \end{bmatrix} \nabla H(q, p) + \begin{bmatrix} 0_{n \times m} \\ G(q) \end{bmatrix} u, \tag{1}$$

where $q, p \in \mathbb{R}^n$ are the generalized position and momenta, respectively, $u \in \mathbb{R}^m$ is the control, $G : \mathbb{R}^n \to \mathbb{R}^{n \times m}$, with $\text{rank}(G) = m < n$, the function $H : \mathbb{R}^n \times \mathbb{R}^n \to \mathbb{R}$,

$$H(q, p) := \frac{1}{2} p^\top M^{-1}(q) \, p + V(q) \tag{2}$$

is the total energy with $M : \mathbb{R}^n \to \mathbb{R}^{n \times n}$, the positive definite mass matrix and $V : \mathbb{R}^n \to \mathbb{R}$ the potential energy.

The control objective is to design a static, state feedback that assigns to the closed loop a desired stable equilibrium $(q, p) = (q^\star, 0)$, $q^\star \in \mathbb{R}^n$. This is achieved in IDA-PBC by matching the pH target dynamics

$$\begin{bmatrix} \dot{q} \\ \dot{p} \end{bmatrix} = \begin{bmatrix} 0_{n \times n} & M^{-1}(q)\, M_d(q) \\ -M_d(q)\, M^{-1}(q) & J_2(q, p) - R_d(q) \end{bmatrix} \nabla H_d, \tag{3}$$

with the new total energy function $H_d : \mathbb{R}^n \times \mathbb{R}^n \to \mathbb{R}$,

$$H_d(q, p) := \frac{1}{2}\, p^\top M_d^{-1}(q)\, p + V_d(q), \tag{4}$$

where the desired mass matrix $M_d : \mathbb{R}^n \to \mathbb{R}^{n \times n}$ is positive definite, the desired potential energy $V_d : \mathbb{R}^n \to \mathbb{R}$ verifies

$$q^\star = \arg\min V_d(q), \tag{5}$$

and the desired damping matix is defined by

$$R_d(q) := G(q) K_P G^\top(q) \geqslant 0,$$

with $K_P \in \mathbb{R}^{m \times m}$ a free positive definite matrix. The matrix $J_2 : \mathbb{R}^n \times \mathbb{R}^n \to \mathbb{R}^{n \times n}$ is free to the designer and fulfills the skew-symmetry condition

$$J_2(q, p) = -J_2^\top(q, p). \tag{6}$$

The closed-loop system (3) has a stable equilibrium point at $(q^\star, 0)$ with Lyapunov function H_d, which verifies

$$\dot{H}_d = -\|G^\top M_d^{-1} p\|_{K_P}^2 \leqslant 0.$$

The closed loop is asymptotically stable provided that the output

$$y_d := G^\top M_d^{-1} p \tag{7}$$

is detectable [16].

By equating the right-hand sides of (1) and (3), one obtains the so-called matching equations, which are two partial differential equations (PDEs) that identify the assignable M_d and V_d and gives an explicit expression for the (static state feedback) control signal $u = u_{\text{IDA}}(q, p)$, where $u_{\text{IDA}} : \mathbb{R}^n \times \mathbb{R}^n \to \mathbb{R}^m$.

2.2. Formulation of the robust interconnection and damping assignment passivity-based control problem

In this paper, we consider the effect of constant, matched disturbances in the mechanical system (1) that may represent external forces or an input measurement bias. We assume that the system (1) is in closed loop with an IDA-PBC into which the disturbance propagates and must be rejected with a dynamic outer-loop control. That is, we consider the system (1) perturbed by an input disturbance in closed loop with the control $u = u_{\text{IDA}}(q, p) + v$, leading to the following.

Problem formulation. Given the dynamics

$$\begin{bmatrix} \dot{q} \\ \dot{p} \end{bmatrix} = \begin{bmatrix} 0_{n \times n} & M^{-1} M_d \\ -M_d M^{-1} & J_2 - G K_P G^\top \end{bmatrix} \nabla H_d + \begin{bmatrix} 0_{n \times m} \\ G \end{bmatrix} (v + d), \tag{8}$$

with H_d as in (4) and $d \in \mathbb{R}^m$. Find (if possible) a dynamic controller $v = \beta(q, p, \zeta)$, where $\zeta \in \mathbb{R}^m$ is the state of the controller, that ensures asymptotic stability of the desired equilibrium $(q, p, \zeta) = (q^\star, 0, \zeta^\star)$, for some $\zeta^\star \in \mathbb{R}^m$, even under the action of constant disturbances d.

Remark 1

Notice that the dimension of the dynamic extension ζ coincides with the one of the input space, that is, m. As will be shown later, this choice suffices to provide a solution to the problem.

3. MAIN RESULT

3.1. The class of mechanical systems

In this section, we present the main result of the paper, which requires the following assumption imposed throughout the rest of the paper.

Assumption A

The input matrix G and the desired mass matrix M_d are constant, and the mass matrix $M(q)$ is independent of the non-actuated coordinates. Consequently,

$$G^\perp \nabla_q (p^\top M^{-1} p) = 0,$$

where $G^\perp \in \mathbb{R}^{(n-m)\times n}$ is a full-rank left-annihilator of G.

Remark 2

The term $G^\perp \nabla_q (p^\top M^{-1} p)$ appears in the kinetic energy matching equation as a forcing term that makes the PDE inhomogeneous and introduces a quadratic term in the unknown M_d, rendering very difficult its solution. In [8], it is also assumed to be zero to provide an explicit solution to the PDE. In [11], changes of coordinates are introduced to eliminate, or simplify, this term. In Proposition 2 of [11], it is shown that a sufficient condition to eliminate this term is that the Coriolis and centrifugal forces of the mechanical system enter into the kernel of G.

Remark 3

Assumption A, which is satisfied by some of the classical benchmark examples, identifies the class of systems for which we provide a solution to the problem formulated in Section 2.2. The relaxation of this assumption is left as an open problem for future research. Some of the classical test beds for which this assumption is not satisfied are, for example, the ball and beam [17], the cart-pole system and the pendubot [18].

3.2. Nonlinear PI controller

Proposition 1

Consider the dynamics (8) with $J_2 = 0$ in closed loop with the PI controller $v = \beta(q, \zeta)$, with

$$\beta(q, \zeta) = = -K_2 K_I K_2^\top G^\top M^{-1} \nabla V_d - K_P K_I \zeta \qquad (9)$$

and

$$\dot{\zeta} = K_2^\top G^\top M^{-1} \nabla V_d, \qquad (10)$$

with constant matrices $K_P > 0$, $K_I > 0$ and

$$K_2 := \left(G^\top M_d^{-1} G \right)^{-1}.$$

P1.1 Introduce the globally defined change of coordinates $z = \psi(q, p, \zeta)$ given by

$$z_1 = q, \qquad (11)$$

$$z_2 = p + G K_2 K_I (\zeta - \alpha), \qquad (12)$$

$$z_3 = \zeta. \qquad (13)$$

The closed-loop dynamics can be written in pH form as follows:

$$\begin{bmatrix} \dot{z}_1 \\ \dot{z}_2 \\ \dot{z}_3 \end{bmatrix} = \begin{bmatrix} 0_{n \times n} & M^{-1} M_d & -M^{-1} G K_2 \\ -M_d M^{-1} & -G K_P G^\top & 0_{n \times m} \\ K_2^\top G^\top M^{-1} & 0_{m \times n} & 0_{m \times m} \end{bmatrix} \nabla H_z, \tag{14}$$

with Hamiltonian

$$H_z(z) = \frac{1}{2} z_2^\top M_d^{-1} z_2 + V_d(z_1) + \frac{1}{2} \|z_3 - \alpha\|_{K_I}^2 \tag{15}$$

and

$$\alpha := (K_P K_I)^{-1} d.$$

P1.2. The equilibrium $(q, p, \zeta) = (q^\star, 0, \alpha)$ is stable.

P1.3. If the output

$$y_{D1} = G^\top M_d^{-1} z_2$$

is a detectable output of the dynamics (14), then $(q^\star, 0, \alpha)$ is an asymptotically stable equilibrium.

Proof

First, to prove **P1.1**, we differentiate (11) to obtain

$$\begin{aligned} \dot{z}_1 &\equiv \dot{q} \\ &= M^{-1} z_2 - M^{-1} G K_2 K_I (z_3 - \alpha), \end{aligned}$$

which allows us to write the first state equation of (14). We proceed in a similar fashion with (12)

$$\begin{aligned} \dot{z}_2 &= \dot{p} + G K_2 K_I \dot{\zeta} \\ &= -M_d M^{-1} \nabla V_d(q) - G K_P G^\top M_d^{-1} p + G(v + d) + G K_2 K_I \dot{\zeta} \\ &= -M_d M^{-1} \nabla V_d(q) - G K_P G^\top M_d^{-1} p + G d \\ &\quad + G \left[-K_2 K_I K_2^\top G^\top M^{-1} \nabla V_d - K_P G^\top M_d^{-1} G K_2 K_I \zeta \right] \\ &\quad + G K_2 K_I K_2^\top G^\top M^{-1} \nabla V_d \big|_{(q,p,\zeta) = \psi^{-1}(z)} \\ &\equiv -M_d M^{-1} \nabla V_d(z_1) - G K_P G^\top M_d^{-1} z_2, \end{aligned}$$

which is the second row of the closed-loop dynamics (14). Finally, we note that the dynamics of ζ and z_3 are equivalent. Indeed, from the last row of (14), we obtain

$$\begin{aligned} \dot{z}_3 &= K_2^\top G^\top M^{-1} \nabla V_d(z_1) \big|_{z = \psi(q,p,\zeta)} \\ &\equiv \dot{\zeta}. \end{aligned}$$

To prove the stability property **P1.2**, we consider H_z as Lyapunov candidate function for the closed loop (14). Its time derivative is as follows:

$$\dot{H}_z = -\|G^\top M_d^{-1} z_2\|_{K_P}^2 \leqslant 0, \tag{16}$$

which ensures stability of the desired equilibrium. The assumption that y_{D1} is a detectable output of the system (14) ensures asymptotic stability of the equilibrium $(q^\star, 0, \alpha)$ [16], proving property **P1.3**. □

Remark 4

The controller (9) is a nonlinear PI (around ∇V_d) of the form

$$v = -\mathcal{K}_P(q)\nabla V_d - \mathcal{K}_I(q)\zeta,$$
$$\dot{\zeta} = \nabla V_d,$$

with nonlinear gains

$$\mathcal{K}_P(q) := K_2 K_I K_2^\top G^\top M^{-1}(q),$$
$$\mathcal{K}_I(q) := K_P K_I K_2^\top G^\top M^{-1}(q).$$

Remark 5

Notice that in the simplest case when V_d is quadratic, that is,

$$V_d(q) = \|q - q^\star\|_S^2,$$

with $S > 0$, then v is a standard PI around the position error $q - q^\star$. This is the case if the system (1) is linear; hence, the gains $\mathcal{K}_P$ and $\mathcal{K}_I$ are constant.

3.3. First nonlinear PID controller

Now, we extend the previous proposition by adding damping in the coordinates z_1 to relax the detectability condition needed to ensure asymptotic stability and simplify its analysis.

Proposition 2

Consider the dynamics (8) with $J_2 = 0$ in closed loop with the PID controller $v = \beta(q, \zeta, p)$, with[‡]

$$\beta(q, \zeta, p) = -\left(K_P G^\top M_d^{-1} G K_1 G^\top M^{-1} + K_1 G^\top \dot{M}^{-1}\right)\nabla V_d \\ - K_1 G^\top M^{-1}\nabla^2 V_d M^{-1} p - K_I \zeta \tag{17}$$

and

$$\dot{\zeta} = G^\top M_d^{-1} G K_1 G^\top M^{-1}\nabla V_d + G^\top M_d^{-1} p, \tag{18}$$

with constant matrices $K_P > 0$, $K_I > 0$ and $K_1 > 0$.

P2.1. The closed-loop dynamics can be written in pH form as follows:

$$\begin{bmatrix} \dot{z}_1 \\ \dot{z}_2 \\ \dot{z}_3 \end{bmatrix} = \begin{bmatrix} -\Gamma_1 & M^{-1}M_d & 0_{n\times m} \\ -M_d M^{-1} & -GK_P G^\top & -G \\ 0_{m\times n} & G^\top & 0_{m\times m} \end{bmatrix} \nabla H_z, \tag{19}$$

with

$$\Gamma_1 := M^{-1}GK_1 G^\top M^{-1} \geqslant 0,$$

Hamiltonian as in (15) and $\alpha := K_I^{-1}d$. The states of (8) and (19) are related by the state transformation $z = \psi(q, p, \zeta)$ as follows:

$$z_1 = q, \tag{20}$$

$$z_2 = p + GK_1 G^\top M^{-1}\nabla V_d, \tag{21}$$

$$z_3 = \zeta. \tag{22}$$

P2.2. The equilibrium $(q, p, \zeta) = (q^\star, 0, \alpha)$ is stable.

[‡]To simplify the notation we use $\dot{M}^{-1}$ to denote $\frac{d(M^{-1})}{dt}$.

P2.3. If the output

$$y_{D2} = \begin{bmatrix} G^\top M^{-1} \nabla V_d \\ G^\top M_d^{-1} z_2 \end{bmatrix}$$

is a detectable output of the dynamics (19), then $(q^\star, 0, \alpha)$ is an asymptotically stable equilibrium of the closed loop.

Proof
First, to prove **P2.1**, we take the state transformation (20), and we differentiate it with respect to time to obtain

$$\begin{aligned} \dot{z}_1 &= -\Gamma_1 \nabla V_d + M^{-1} z_2 \\ &= -\Gamma_1 \nabla V_d + M^{-1} [p + M\Gamma_1 \nabla V_d] \\ &\equiv \dot{q}, \end{aligned}$$

which allows us to write the first state equation of (14). We proceed in a similar fashion with the state transformation (21). By differentiating with respect to time, we obtain

$$\begin{aligned} \dot{z}_2 &= \dot{p} + GK_1 G^\top M^{-1} \nabla^2 V_d \dot{q} + GK_1 G^\top \dot{M}^{-1} \nabla V_d \\ &= -M_d M^{-1} \nabla V_d(q) - GK_P G^\top M_d^{-1} p + G(v + d) + GK_1 G^\top M^{-1} \nabla^2 V_d M^{-1} p \\ &\quad + GK_1 G^\top \dot{M}^{-1} \nabla V_d \\ &= -M_d M^{-1} \nabla V_d(q) - GK_P G^\top M_d^{-1} p + Gd + G\left[-K_P G^\top M_d^{-1} GK_1 G^\top M^{-1} \nabla V_d \right. \\ &\quad \left. -K_I \zeta - K_1 G^\top M^{-1} \nabla^2 V_d M^{-1} p - K_1 G^\top \dot{M}^{-1} \nabla V_d \right] + GK_1 G^\top M^{-1} \nabla^2 V_d M^{-1} p \\ &\quad + GK_1 G^\top \dot{M}^{-1} \nabla V_d \\ &= -M_d M^{-1} \nabla V_d(q) - GK_P G^\top M_d^{-1} \left[p + GK_1 G^\top M^{-1} \nabla V_d \right] \\ &\quad -GK_I (\zeta - \alpha)|_{(q,p,\zeta) = \psi^{-1}(z)} \\ &\equiv -M_d M^{-1} \nabla V_d(z_1) - GK_P G^\top M_d^{-1} z_2 - GK_I (z_3 - \alpha), \end{aligned}$$

which is the second row of the closed-loop dynamics (19). Finally, we note that the dynamics of ζ and z_3 are equivalent. Indeed, from the last row of (19), we obtain

$$\begin{aligned} \dot{z}_3 &= G^\top M_d^{-1} z_2 \big|_{z = \psi(q,p,\zeta)} \\ &\equiv \dot{\zeta}. \end{aligned}$$

The proof of **P2.2** and **P2.3** mimics the proof of Proposition 1, noting that

$$\dot{H}_z = -\|G^\top M^{-1} \nabla V_d\|_{K_1}^2 - \|G^\top M_d^{-1} z_2\|_{K_P}^2.$$

$\square$

Remark 6
The controller (17) differs from the nonlinear PI (9) in two respects. First, it contains a derivative term with respect to the signal ∇V_d—hence, the addition of the letter D to the PI name. Second, besides the integral action (around ∇V_d), there is another one around $\dot{q}$. Indeed, (17) can be written in the form

$$\begin{aligned} v &= -\mathcal{K}_P(q, \dot{q}) \nabla V_d - \zeta_1 - \zeta_2 - \mathcal{K}_D(q) \frac{d\nabla V_d}{dt}, \\ \dot{\zeta}_1 &= \mathcal{K}_{I1}(q) \nabla V_d, \\ \dot{\zeta}_2 &= \mathcal{K}_{I2}(q) \dot{q}, \end{aligned}$$

with some suitable nonlinear gains $\mathcal{K}_P(q, \dot{q})$, $\mathcal{K}_D(q)$ and $\mathcal{K}_{Ii}(q)$, $i = 1, 2$, defined as follows:

$$
\begin{aligned}
\mathcal{K}_P(q, \dot{q}) &= K_P G^\top M_d^{-1} G K_1 G^\top M^{-1} + K_1 G^\top \dot{M}^{-1}, \\
\mathcal{K}_D(q) &= K_1 G^\top M^{-1}, \\
\mathcal{K}_{I1}(q) &= K_I^{-1} G^\top M_d^{-1} G K_1 G^\top M^{-1}, \\
\mathcal{K}_{I2}(q) &= K_I^{-1} G^\top M_d^{-1} M.
\end{aligned}
$$

Remark 7

It is important to underscore the presence of the positive semidefinite matrix Γ_1 in the $(1, 1)$ block of the system matrix in (19). This additional damping term allows—via the addition of the term $G^\top M^{-1} \nabla V_d$ in y_{D2}—to relax the condition P1.3 for asymptotic stability.

3.4. Second nonlinear PID controller

We present now a more elaborated nonlinear PID controller with the following features:

- To simplify the asymptotic stability analysis, it adds damping in coordinates z_3, as well as in z_1 and z_2.
- The assumption of $J_2 = 0$ is obviated, enlarging the class of closed-loop systems (8) to be considered.

Proposition 3

Consider the dynamics (8) in closed-loop with the PID controller $v = \beta(q, \zeta, p)$, with

$$
\begin{aligned}
\beta(q, \zeta, p) = &-\left[K_p G^\top M_d^{-1} G K_1 G^\top M^{-1} + K_1 G^\top \dot{M}^{-1} + K_2 K_I \right. \\
&\left. \times \left(K_2^\top + K_3^\top G^\top M_d^{-1} G K_1 \right) G^\top M^{-1} \right] \nabla V_d \\
&-\left[K_1 G^\top M^{-1} \nabla^2 V_d M^{-1} + (G^\top G)^{-1} G^\top J_2 M_d^{-1} + K_2 K_I K_3^\top G^\top M_d^{-1} \right] p \\
&-\left(K_P G^\top M_d^{-1} G K_2 + K_3 \right) K_I \zeta
\end{aligned}
\tag{23}
$$

and

$$
\dot{\zeta} = \left(K_2^\top G^\top M^{-1} + K_3^\top G^\top M_d^{-1} G K_1 G^\top M^{-1} \right) \nabla V_d + K_3^\top G^\top M_d^{-1} p,
\tag{24}
$$

where $K_1 > 0$, $K_P > 0$, and $K_I > 0$, $K_3 > 0$ and

$$
K_2 := \left(G^\top M_d^{-1} G \right)^{-1}.
$$

P3.1. The closed-loop dynamics can be written in pH form as follows:

$$
\begin{bmatrix} \dot{z}_1 \\ \dot{z}_2 \\ \dot{z}_3 \end{bmatrix} =
\begin{bmatrix} -\Gamma_1 & M^{-1} M_d & -\Gamma_2 \\ -M_d M^{-1} & -G K_P G^\top & -G K_3 \\ \Gamma_2^\top & K_3^\top G^\top & -K_3^\top \end{bmatrix} \nabla H_z
\tag{25}
$$

with Hamiltonian as in (15), and the constant gains

$$
\begin{aligned}
\Gamma_1 &:= M^{-1} G K_1 G^\top M^{-1}, \\
\Gamma_2 &:= M^{-1} G K_2, \\
\alpha &:= K_I^{-1} (K_P + K_3)^{-1} d.
\end{aligned}
$$

The states of (8) and (25) are related by the state transformation $z = \psi(q, p, \zeta)$ as follows:

$$
z_1 = q,
\tag{26}
$$

$$
z_2 = p + G K_1 G^\top M^{-1} \nabla V_d(q) + G K_2 K_I (\zeta - \alpha),
\tag{27}
$$

$$z_3 = \zeta. \tag{28}$$

P3.2. The equilibrium $(q, p, \zeta) = (q^\star, 0, \alpha)$ is stable.

P3.3. If the output

$$y_{D3} = \begin{bmatrix} G^\top M^{-1}\nabla V_d \\ G^\top M_d^{-1} z_2 \\ K_I(z_3 - \alpha) \end{bmatrix}$$

is a detectable output of the dynamics (25), then $(q^\star, 0, \alpha)$ is an asymptotically stable equilibrium of the closed loop.

Proof

We proceed as in the proof of previous propositions, to prove **P3.1**, we take the state transformation (26), and we differentiate it with respect to time to obtain

$$
\begin{aligned}
\dot{z}_1 &= -\Gamma_1 \nabla_{z_1} V_d(z_1) + M^{-1} z_2 - \Gamma_2 K_I(z_3 - \alpha) \\
&= -\Gamma_1 \nabla_{z_1} V_d(z_1) + M^{-1} \left[p + G K_1 G^\top M^{-1} \nabla V_d + G K_2 K_I(\zeta - \alpha) \right] \\
&\quad -\Gamma_2 K_I(z_3 - \alpha)\big|_{z_1 = q} \\
&\equiv \dot{q},
\end{aligned}
\tag{29}
$$

which allows us to write state first state equation of (25). Similarly, we take the state transformation (27), and we differentiate it with respect to time to obtain

$$
\begin{aligned}
\dot{z}_2 &= \dot{p} + G K_1 G^\top \dot{M}^{-1} \nabla V_d + G K_1 G^\top M^{-1} \nabla^2 V_d \dot{q} + G K_2 K_I \dot{\zeta} \\
&= -M_d M^{-1} \nabla V_d(q) + \left(J_2 - G K_P G^\top \right) M_d^{-1} p + G\, v + G\, d \\
&\quad + G K_1 G^\top \dot{M}^{-1} \nabla V_d + G K_1 G^\top M^{-1} \nabla^2 V_d M^{-1} p + G K_2 K_I \dot{\zeta} \\
&= -M_d M^{-1} \nabla V_d + \left(J_2 - G K_P G^\top \right) M_d^{-1} p + G d \\
&\quad + G \left[-K_P G^\top M_d^{-1} G K_1 G^\top M^{-1} \nabla V_d - K_1 G^\top \dot{M}^{-1} \nabla V_d \right. \\
&\quad - \left(K_1 G^\top M^{-1} \nabla^2 V_d M^{-1} \right) p - (G^\top G)^{-1} G^\top J_2 M_d^{-1} p - K_2 K_I \dot{\zeta} \\
&\quad - \left. \left(K_P G^\top M_d^{-1} G K_2 + K_3 \right) K_I \zeta \right] + G K_1 G^\top M^{-1} \nabla^2 V_d M^{-1} p \\
&\quad + G K_1 G^\top \dot{M}^{-1} \nabla V_d + G K_2 K_I \dot{\zeta}\Big|_{(q,p,\zeta)=\psi^{-1}(z)} \\
&\equiv -M_d M^{-1} \nabla V_d(z_1) - G K_P G^\top M_d^{-1} z_2 - G K_3 K_I(z_3 - \alpha),
\end{aligned}
\tag{30}
$$

which is the second row of the closed-loop dynamics (25). Finally, from the last row of (25), we note that the dynamics of ζ and z_3 are equivalent, that is,

$$
\begin{aligned}
\dot{z}_3 &= \Gamma_2^\top \nabla V_d(z_1) + K_3^\top G^\top M_d^{-1} z_2 - K_3^\top K_I(z_3 - \alpha)\big|_{z=\psi(q,p,\zeta)} \\
&= K_2^\top G^\top M^{-1} \nabla V_d + K_3^\top G^\top M_d^{-1} \left[p + G K_1 G^\top M^{-1} \nabla V_d \right. \\
&\quad + \left. G K_2 K_I(\zeta - \alpha) \right] - K_3^\top K_I(\zeta - \alpha) \\
&\equiv \dot{\zeta}.
\end{aligned}
\tag{31}
$$

The stability property **P3.2** follows from

$$\dot{H}_z = -\|G^\top M^{-1} \nabla V_d(z_1)\|_{K_1}^2 - \|G^\top M_d^{-1} z_2\|_{K_P}^2 - \|K_I(z_3 - \alpha)\|_{K_3}^2 \leqslant 0. \tag{32}$$

The assumption that y_{D3} is a detectable output of the system (25) ensures asymptotic stability of the equilibrium $(q^\star, 0, \alpha)$ [16], proving property **P3.3**. $\qquad\square$

Remark 8

Note that the controller in Proposition 1 can be derived from the one in Proposition 3 setting $K_1 = 0$ and $K_3 = 0$. An extra term needs to be added to deal with the case when $J_2 \neq 0$. Similarly, the controller in Proposition 2 can be derived from the one in Proposition 3 by setting $K_2 = 0$ and $K_3 = I_m$, and including a term to handle $J_2 \neq 0$.

4. THE ACROBOT EXAMPLE

In this section, we consider the example of the Acrobot studied in [19]. The IDA-PBC controller used in this section was borrowed from [9]. It is interesting to note that all the mechanical systems studied in [9], including the Acrobot, belong to the class of systems we consider in our work.

4.1. Dynamic model and interconnection and damping assignment passivity-based control

The equations of motion of the Acrobot are given by (1) with $n = 1, m = 1$,

$$M(q_2) = \begin{bmatrix} c_1 + c_2 + 2c_3 \cos(q_2) & c_2 + c_3 \cos(q_2) \\ c_2 + c_3 \cos(q_2) & c_2 \end{bmatrix},$$
$$V(q) = g \left[c_4 \cos(q_1) + c_5 \cos(q_1 + q_2) \right],$$
$$G = \begin{bmatrix} 0 \\ 1 \end{bmatrix},$$

where g is the gravitational constant, and c_1, c_2, c_3 and c_4 are constant parameters of the system with $c_1 \neq c_2$.

The upright equilibrium $q^\star = (0,0)$ of the Acrobot can be stabilized asymptotically with the IDA-PBC controller

$$u_{\text{IDA}}(q, p) = \frac{1}{2} \nabla_{q_2} (p^\top M^{-1} p) + \nabla_{q_2} V - \begin{bmatrix} k_2 & k_3 \end{bmatrix} M^{-1} \nabla V_d$$
$$+ \frac{k_v}{k_1 k_3 - k_2^2} (k_2 p_1 - k_1 p_2),$$

where $k_v > 0$ is the damping injection gain, and the controller gains k_1, k_2, and k_3 with

$$k_1 := \left(1 - \sqrt{c_1/c_2}\right) k_2 > 0,$$

and

$$k_3 > \frac{k_2}{1 - \sqrt{c_1/c_2}}.$$

The desired mass matrix is

$$M_d = \begin{bmatrix} k_1 & k_2 \\ k_2 & k_3 \end{bmatrix} > 0,$$

and the desired potential energy is such that

$$\nabla_{q_1} V_d = -k_0 \sin(q_1 - \mu q2) - b_1 \sin(q_1) - b_2 \sin(q_1 + q_2) - b_3 \sin(q_1 + 2q_2)$$
$$- b_4 \sin(q_1 - q_2) + k_u(q_1 - \mu q_2),$$
$$\nabla_{q_2} V_d = k_0 \mu \sin(q_1 - \mu q_2) - b_2 \sin(q_1 + q_2) - 2b_3 \sin(q_1 + 2q_2) + b_4 \sin(q_1 - q_2) -$$
$$- k_u \mu (q_1 - \mu q_2),$$

with the constants

$$b_1 := \frac{g}{2k_2} \left(c_3 c_5 \pm 2\sqrt{c_1 c_2} c_4 \right), \ b_2 := \frac{g\mu}{2k_2(\mu + 1)} \left(c_3 c_4 \pm 2\sqrt{c_1 c_2} c_5 \right)$$
$$b_3 := \frac{g\mu c_3 c_5}{2k_2(\mu + 2)}, \ b_4 := \frac{g\mu c_3 c_4}{2k_2(\mu - 1)}, \ \mu := \frac{-1}{1 + \sqrt{\frac{c_1}{c_2}}}, k_u > k_0 + g^2(c_4 + c_5)^2 \rho,$$

and arbitrary constant k_0.

Remark 9

It is important to underscore that the IDA-PBC given earlier ensures asymptotic stability of the upward Acrobot position with a domain of attraction including a region in the lower half plane, that is, $|q_1| > \frac{\pi}{2}$. That is, the IDA-PBC can swing up the Acrobot without switching. To the best of the authors' knowledge, this is the first such result for any pendular system. See [9] for further details of the controller design and the stability proof.

4.2. Simulations of the perturbed system with interconnection and damping assignment passivity-based control only

To assess the effect of the external disturbance, some simulations were carried out. For the simulations, we use the values of the model parameters provided in [9], that is, $g = 9.8$, $c_1 = 2.3333$, $c_2 = 5.3333$, $c_3 = 2$, $c_4 = 3$, $c_5 = 2$. The gains of the IDA-PBC without the PID were selected as follows: $k_1 = 0.3386$, $k_2 = 1$, $k_3 = 5.9073$, $\mu = -0.6019$, $k_0 = -350$, $k_u = 10$, and $k_v = 70$.

The simulations are performed under the following extreme scenario: the system starts with the Acrobot in closed loop with the IDA-PBC hanging down with zero velocity, that is with initial conditions $q_1(0) = -\pi$, $q_2(0) = 0$, $p_1(0) = 0$ and $p_2(0) = 0$ and without any disturbance. Then, a matched constant disturbance $d = 10$ Nm is added to actuated link of the system at time $t = 25$ s (Figure 5). Figures 1 and 2 show the time histories of the angles and angular velocities of the Acrobot when only the IDA-PBC is used. As expected, the presence of the disturbance
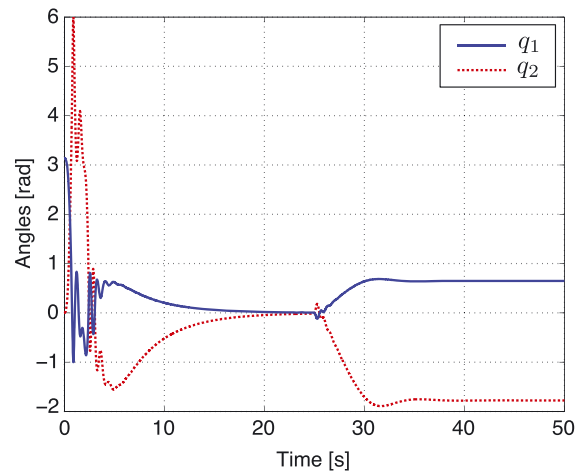

Figure 1. Time histories of the Acrobot angles q_1 and q_2 with IDA-PBC only.
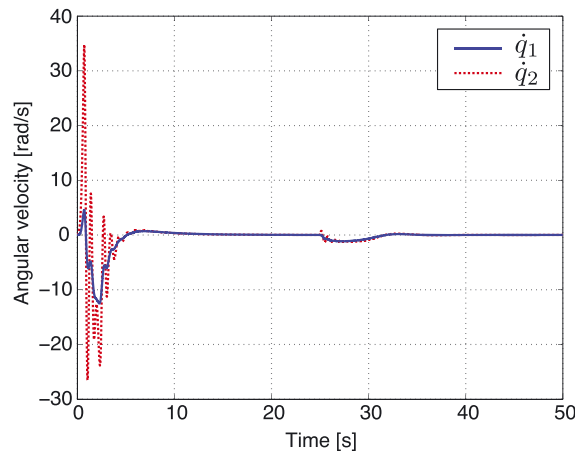

Figure 2. Time histories of the Acrobot angular velocities $\dot{q}_1$ and $\dot{q}_2$ with the IDA-PBC only.

produces an error on the regulation task by shifting the equilibrium of the closed loop from the desired equilibrium.

4.3. Simulations of the perturbed system with interconnection and damping assignment passivity-based control and nonlinear PID outer-loop

First, we observe that G and the desired mass matrix are constant and $G^\perp \nabla_q(p^\top M^{-1} p) = 0$, thus **Assumption A** is verified. To reject the disturbances, we add to the IDA-PBC the outer-loop controller (23), (24) of Proposition 3 with the parameters K_1, K_3, K_I and K_P to be chosen.

To achieve better performance when we add the nonlinear PID controller (23), (24) in the loop, the gains of the IDA-PBC were retuned. In this case, the gains were selected as follows: $k_1 = 0.3386$, $k_2 = 1, k_3 = 5.9073, \mu = -0.6019, k_0 = -260, k_u = 60, k_v = 70, K_1 = 0.005, K_3 = 25, K_I = 0.02$, and $K_P = k_v$. The controller parameters were selected by simulating the closed loop and choosing those that achieve good performance. Clearly, it is also possible to use the more systematic and classical technique of evaluation of the eigenvalues of the linearized closed-loop system, but this turned out to be unnecessary. It should be mentioned that there are some advanced techniques to carry out the IDA-PBC design ensuring that the linearisation of the closed-loop dynamics has, indeed, the desired eigenvalues [20].

In a second test, we simulate, under the same scenario as before, the Acrobot in closed loop with the IDA-PBC augmented with the nonlinear PID controller (23), (24). Figures 3 and 4
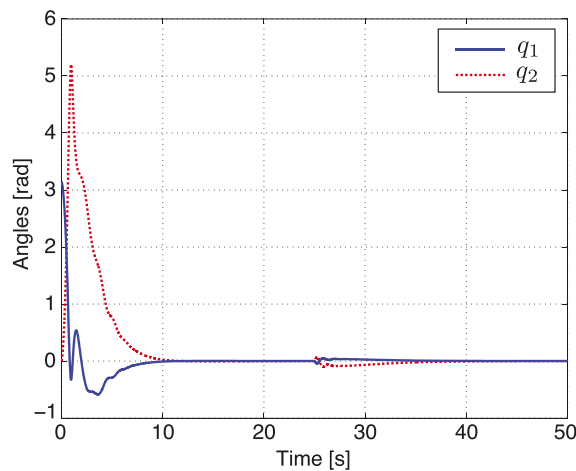

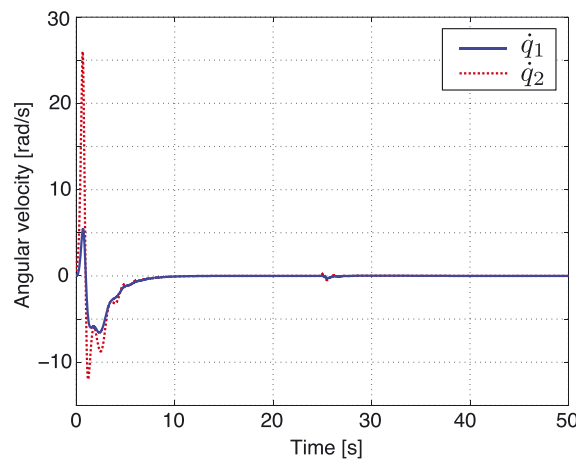Figure 3. Time histories of the Acrobot angles q_1 and q_2 with the IDA-PBC plus the nonlinear PID.

Figure 4. Time histories of the Acrobot angular velocities $\dot{q}_1$ and $\dot{q}_2$ with the IDA-PBC plus the lnonlinear PID.
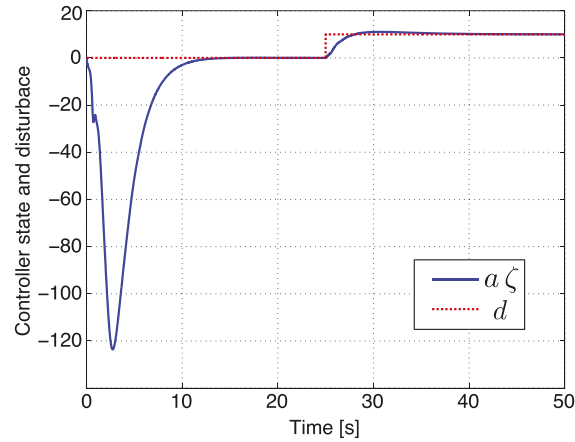
Figure 5. Time history of the matched disturbance d, and the controller state ζ multiplied by the constant $a = (K_P + K_3) K_I$.
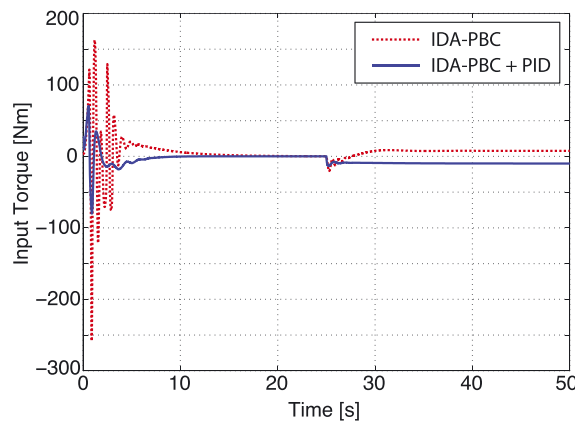

Figure 6. Time history of the control signal u for IDA-PBC with and without the PID.

show the time histories of the Acrobot's angles and angular velocities. It is clear, from the plots, that the angles converge to the desired position, while the velocities converge to zero. Figure 5 shows the time history of the controller state ζ, which provides the disturbance rejection. Note that the plot of ζ in Figure 5 has been multiplied by the constant $a = (K_P + K_3) K_I$, such that $a \zeta$ converges to $a \alpha = d$. The time history of the control input u is shown in Figure 6 for the IDA-PBC with and without the nonlinear PID controller.

A video animation of the Acrobot in closed loop with both IDA-PBC and IDA-PBC plus the PID controller can be watched on `https://youtu.be/JWqGukrjs44`. The simulations and animations were performed under the same scenario, which was previously described in this section.

5. EXPERIMENTS ON THE DISK-ON-DISK

5.1. Dynamic model and interconnection and damping assignment passivity-based control

In this section, we show experiments of an IDA-PBC with and without the nonlinear PID outer-loop controller for the disk-on-disk system shown in Figure 7. This system consist of a non-actuated disk that rolls without slipping on another disk, which is actuated (see [21] for details of the model). The coordinates of the systems are $q = [q_1, q_2]$, where q_1 is the angle of the actuated disk, and q_2 is the deviation angle of the non-actuated disk respect to the upright position. The mass matrix, the input matrix and the potential energy of the system are as follows:
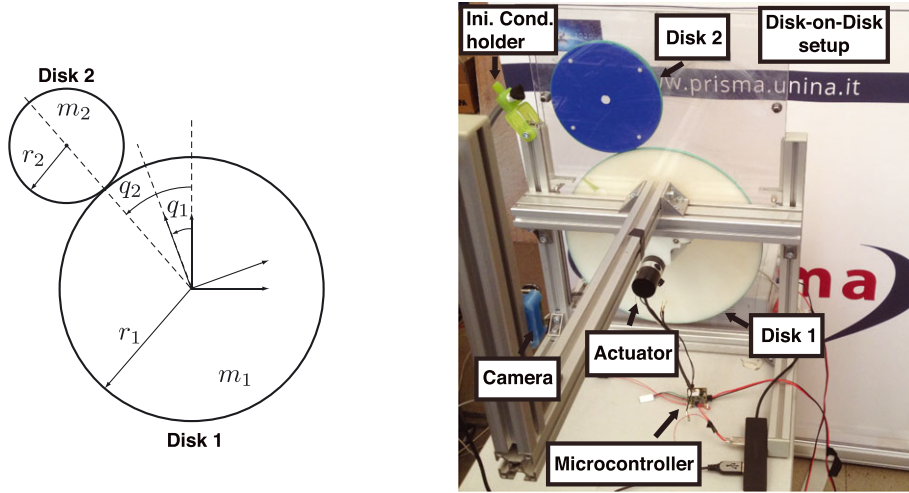
Figure 7. Idealized scheme of the disk-on-disk system and real setup.

$$M = \begin{bmatrix} m_{11} & m_{12} \\ m_{21} & m_{22} \end{bmatrix}, \quad G = \begin{bmatrix} 1 \\ 0 \end{bmatrix}, \quad V = m_2 g(r_1 + r_2) \cos(q_2), \qquad (33)$$

with $m_{11} = r_1^2 (m_1 + m_2)$, $m_{12} = -m_2 r_1 (r_1 + r_2)$, and $m_{22} = 2m_2 (r_1 + r_2)^2$. The parameters m_i and r_i are the mass and radius of the disk i, respectively, for $i = 1, 2$. The constant g is the gravity.

The control objective is to stabilize the desired equilibrium $q^\star = (0, 0)$, which is open-loop unstable. Using the classical IDA-PBC method, we obtain the controller

$$u_{\text{IDA}}(q, p) = \alpha_1 m_1 g(r_1 + r_2) \sin(q_2) - \alpha_2 (q_1 - \alpha_3 q_2) - \frac{k_v}{k_1 k_2 - k_3^2} (k_3 p_1 - k_2 p_2), \qquad (34)$$

where

$$\alpha_1 := \frac{k_2 m_{11} - k_1 m_{12}}{k_3 m_{11} - k_2 m_{12}}, \quad \alpha_2 := k_4 \left(\frac{k_1 k_3 - k_2^2}{k_3 m_{11} - k_2 m_{12}} \right), \quad \alpha_3 := \frac{k_2 m_{22} - k_3 m_{12}}{k_3 m_{11} - k_2 m_{12}},$$

the damping injection gain $k_v > 0$, and the controller parameters k_1, k_2, k_3, and k_4 that satisfy

$$k_1 > 0, \quad k_1 k_3 - k_2^2 > 0, \quad k_4 > 0, \quad k_2 m_{12} - k_3 m_{11} > 0. \qquad (35)$$

The desired mass matrix is

$$M_d = \begin{bmatrix} k_1 & k_2 \\ k_2 & k_3 \end{bmatrix} > 0,$$

and the desired potential energy is

$$V_d(q) = -\alpha_4 m_2 g(r_1 + r_2) \cos(q_2) + \frac{k_4}{2} (q_1 - \alpha_3 q_2)^2, \qquad (36)$$

with $\alpha_4 = \frac{k_3 m_{11} - k_2 m_{12}}{m_{11} m_{22} - m_{12}^2}$.

5.2. *Nonlinear PID outer loop: experiments*

We first notice that the disk-on-disk verifies **Assumption A**. Thus, to reject the disturbances, we add to the IDA-PBC the outer-loop controller (23), (24) of Proposition 3 with the parameters K_1, K_3, K_I, and K_P to be chosen.
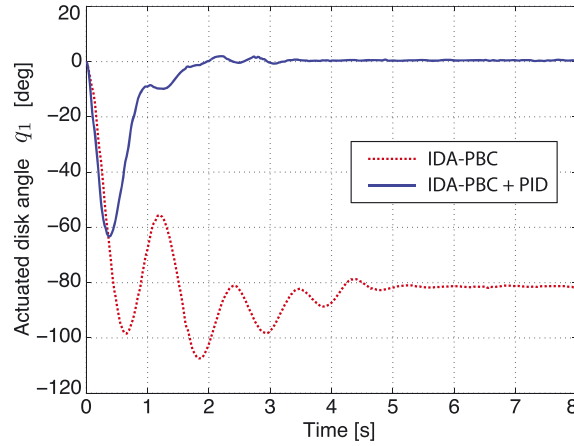
Figure 8. Time history of coordinate q_1 with the IDA-PBC controller only and the IDA-PBC plus the nonlinear PID. The initial condition is set to $q_1(0) = 0$ deg.
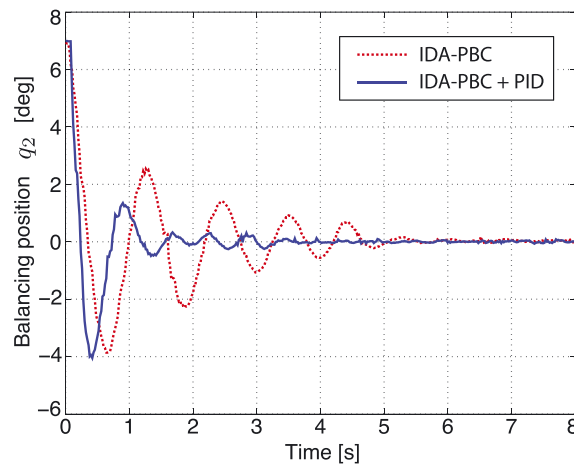

Figure 9. Time history of the coordinate q_2 with the IDA-PBC controller only and the IDA-PBC plus the nonlinear PID. The initial condition is set to $q_2(0) = 7$ deg.

We carry out some experiments to evaluate the performance of the IDA-PBC controller and the IDA-PBC plus the nonlinear PID (23)–(24) in the real setup shown in Figure 7. The model parameters are $m_1 = 0.235$ kg, $m_2 = 0.0216$ kg, $r_1 = 0.15$ m, and $r_2 = 0.075$ m. The parameters of the IDA-PBC controller without PID were selected as follows: $k_1 = 0.4$, $k_2 = -0.03$, $k_3 = 0.003$, $k_4 = 0.00005$, and $k_v = 0.8$. The parameters of the IDA-PBC controller with the PID were chosen as follows: $k_1 = 0.4$, $k_2 = -0.03$, $k_3 = 0.003$, $k_4 = 0.00025$, $k_v = 0.3$, $K_1 = 0.012$, $K_3 = 0.06$, $K_I = 2.2$, and $K_P = k_v$.

In the experiment, we add a matched constant disturbance to the system of value $d = 0.01$ Nm. Figures 8 and 9 show the time history of the angle of the disk q_1 and the balancing angle q_2, respectively. The plot in Figure 8 evidences that both controllers are able to balance the non-actuated disk at the upright position, which is confirmed by the fact that q_2 converges to zero. However, the action of the disturbance deteriorate the performance of the IDA-PBC controller and produces a shift of the desired equilibrium angle of the actuated disk, which does not converge to zero as desired as shown in Figure 9. This figure also shows that the outer nonlinear PID compensate the disturbance and clearly improve the performance of the IDA-PBC controller. The state of the controller ζ is shown in Figure 10 together with the disturbance, which shows that effectively the nonlinear PID compensates the action of the disturbance. Finally, the time history of the control input is depicted in Figure 11, which shows that the controller produces a physically reasonable torque.
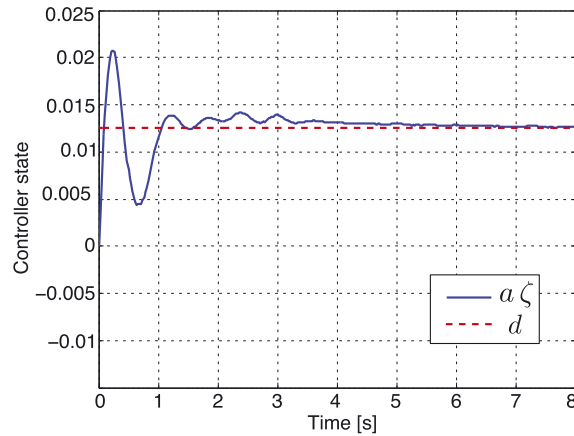
Figure 10. Time history of the matched disturbance d and the controller state ζ multiplied by the constant $a = (K_P + K_3) K_I$.
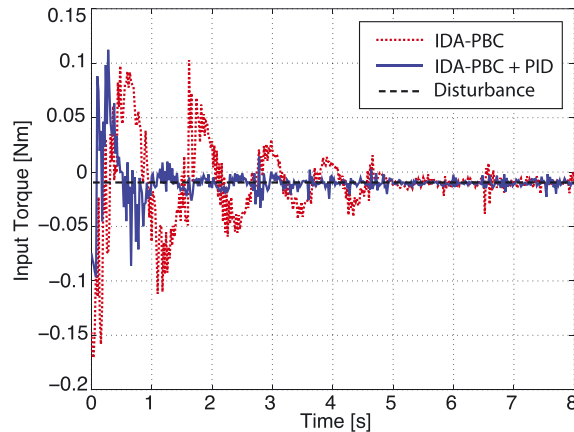

Figure 11. Time history of the control input for the IDA-PBC with and without the nonlinear PID and the disturbance with the sign changed.

A video of the experiments of the disk-on-disk system in closed loop with IDA-PBC with and without the nonlinear PID controller can be watched on `https://youtu.be/JWqGukrjs44`.

6. CONCLUSIONS

In this paper we presented an outer-loop control design to improve the robustness of IDA-PBC for underactuated mechanical system subject to matched constant disturbances. First, it is shown that a nonlinear PI ensures stability of the desired equilibrium and, under some additional assumption, also asymptotic stability. To relax the latter assumption, enlarging the class of systems for which convergence is ensured, additional damping terms are added to the closed loop. This leads to the inclusion of a derivative term in the control law, yielding a nonlinear PID.

In future work, we attempt to relax **Assumption A**, that imposes serious constraints on the class of systems for which IDA-PBC is applicable. Also, in the spirit of [12], we are considering the presence of matched and unmatched disturbances simultaneously, which might be possibly time-varying.

REFERENCES

1. Ortega R, van der Schaft A, Mareels I, Maschke B. Putting energy back in control. *IEEE Control Systems Magazine* 2001; **21**(2):18–33.

2. Aoki T, Yamashita Y, Tsubakino D. Vibration suppression for mass-spring-damper systems with a tuned mass damper using interconnection and damping assignment passivity-based control. *International Journal of Robust and Nonlinear Control* 2016; **26**(2):235–251.

3. Ramirez H, Le Gorrec YL, Macchelli A, Zwart H. Exponential stabilization of boundary controlled port-Hamiltonian systems with dynamic feedback. *IEEE Transactions on Automatic Control* 2014; **59**(10):2849–2855.

4. Cai Z, Qu W, Xi Y, Wang Y. Stabilization of an underactuated bottom-heavy airship via interconnection and damping assignment. *International Journal of Robust and Nonlinear Control* 2007; **17**(18):1690–1715.

5. Ramirez H, Le Gorrec YL, Maschke B, Couenne F. On the passivity based control of irreversible processes: a port-Hamiltonian approach. *Automatica* 2016; **64**(1):105–111.

6. Shimizu T, Kobayashi Y, Sasaki M, Okada T. Passivity-based control of a magnetically levitated flexible beam. *International Journal of Robust and Nonlinear Control* 2009; **19**(6):662–675.

7. Ortega R, Garcia-Canseco E. Interconnection and damping assignment passivity-based control: A survey. *European Journal of Control* 2004; **10**(5):432–450.

8. Acosta J, Ortega R, Astolfi A, Mahindrakar A. Interconnection and damping assignment passivity-based control of mechanical systems with underactuation degree one. *IEEE Transactions on Automatic Control* 2005; **50**(12): 1936–1955.

9. Mahindrakar A, Astolfi A, Ortega R, Viola G. Further constructive results on interconnection and damping assignment control of mechanical systems: the Acrobot example. *International Journal of Robust and Nonlinear Control* 2006; **16**(14):671–685.

10. Ortega R, Spong M, Gomez-Estern F, Blankenstein G. Stabilization of a class of underactuated mechanical systems via interconnection and damping assignment. *IEEE Transactions on Automatic Control* 2002; **47**(8):1218–1233.

11. Viola G, Ortega R, Banavar R, Acosta J, Astolfi A. Total energy shaping control of mechanical systems: simplifying the matching equations via coordinate changes. *IEEE Transactions on Automatic Control* 2007; **52**(6):1093–1099.

12. Romero J, Donaire A, Ortega R. Robust energy shaping control of mechanical systems. *Systems & Control Letters* 2013; **62**(9):770–780.

13. Donaire A, Junco S. On the addition of integral action to port-controlled Hamiltonian systems. *Automatica* 2009; **45**:1910–1916.

14. Dirksz D, Scherpen J. Power-based control: canonical coordinate transformations, integral and adaptive control. *Automatica* 2012; **48**(6):1045–1056.

15. Ryalat M, Laila D, Torbati M. Integral IDA-PBC and PID-like control for port-controlled Hamiltonian systems. In *2015 American Control Conference*, Chicago, IL, USA, 2015; 5365–5370.

16. van der Schaft A. L_2-*Gain and Passivity Techniques in Nonlinear Control*. Springer-Verlag: Berlin, 2000.

17. Hause J, Sastry S, Kokotovic P. Nonlinear control via approximate input–ouput linearisation: the ball and beam example. *IEEE Transactions on Automatic Control* 1992; **37**(3):392–398.

18. Spong M, Block D. The Pendubot: A mechatronic system for control research and education. In *The IEEE Conference on Decision and Control*, New Orleans, LA, USA, 1995; 555–557.

19. Spong M. The swing-up control problem for the Acrobot. *IEEE Control Systems Magazine* 1995; **15**(1):49–55.

20. Kotyczka P. Local linear dynamics assignment in IDA-PBC. *Automatica* 2013; **49**(4):1037–1044.

21. Ryu J-C, Ruggiero F, Lynch KM. Control of nonprehensile rolling manipulation: balancing a disk on a disk. *IEEE Transactions on Robotics* 2013; **29**(5):1152–1161.